Accepted Manuscript

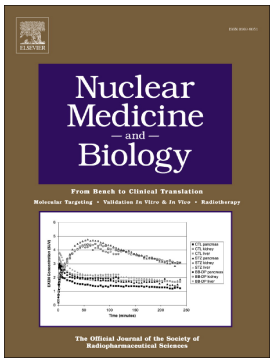

[18F]diphenyl sulfide derivatives for imaging serotonin transporter (SERT) in the brain

Yan Zhang, Futao Liu, Hao Xiao, Xinyue Yao, Genxun Li, Seok Rye Choi, Karl Ploessl, Zhihao Zha, Lin Zhu, Hank F. Kung

PII: S0969-8051(18)30054-4
DOI: doi:10.1016/j.nucmedbio.2018.06.008
Reference: NMB 8026

To appear in: *Nuclear Medicine and Biology*

Received date: 15 February 2018
Revised date: 15 June 2018
Accepted date: 28 June 2018

Please cite this article as: Yan Zhang, Futao Liu, Hao Xiao, Xinyue Yao, Genxun Li, Seok Rye Choi, Karl Ploessl, Zhihao Zha, Lin Zhu, Hank F. Kung , [18F]diphenyl sulfide derivatives for imaging serotonin transporter (SERT) in the brain. Nmb (2018), doi:10.1016/j.nucmedbio.2018.06.008

[^{18}F]Diphenyl Sulfide Derivatives for Imaging Serotonin Transporter (SERT) in the Brain

Yan Zhang,[a] Futao Liu,[a,c] Hao Xiao,[a] Xinyue Yao,[a] Genxun Li,[a] Seok Rye Choi,[c] Karl Ploessl,[c] Zhihao Zha[b], Lin Zhu,[a,b*] Hank F. Kung[b,c*]

[a]Key Laboratory of Radiopharmaceuticals (College of Chemistry, Beijing Normal University), Ministry of Education, Beijing, 100875, China

[b]Beijing Institute for Brain Disorders, Capital Medical University, Beijing, 100069, China

[c]Department of Radiology, University of Pennsylvania, Philadelphia, PA 19104, USA

Total pages: 34, Word count: 8284, Schemes: 1, Figures: 6, Tables: 3

[*]Corresponding author contact information:

Hank F. Kung, PhD, Department of Radiology, University of Pennsylvania, 3700 Market Street, Room 305, Philadelphia, PA 19104, USA

Tel.: +1 215 662 3989; fax: +1 215 349 5035; email: Kunghf@gmail.com

Lin Zhu, PhD, Key Laboratory of Radiopharmaceuticals (Beijing Normal University), Ministry of Education, No. 19, XinJieKouWai Street, Haidian District, Beijing, 100875, P. R. China

Tel.: +86 10 62200772; email: zhulin@bnu.edu.cn

Abstract

Objectives: Serotonin transporters (SERT) play an important role in controlling serotonin concentration in the synaptic cleft and in managing postsynaptic signal transduction. Inhibitors of SERT binding are well known as selective serotonin reuptake inhibitors (SSRIs) such as fluoxetine, sertraline, paroxetine, and escitalopram, that are commonly prescribed antidepressants. Positron emission tomography (PET) and single photon emission tomography (SPECT) imaging agents targeting SERT may be useful for studying its function and providing a tool for monitoring drug treatment.

Methods: A series of novel ^{18}F-labeled diphenyl sulfide derivatives were prepared and tested for their binding affinity. Among them, 2-((2-((dimethylamino)-methyl)-4-(2-(2-fluoroethoxy)ethoxy)phenyl)thio)aniline, **1**, which showed excellent binding toward serotonin transporter (SERT) in the brain (K_i = 0.09 nM), was selected for further evaluation. An active OTs intermediate, **7**, was treated with [^{18}F]F^-/K_{222} to provide [^{18}F]**1** in one step and in high radiochemical yields. This new SERT targeting agent was evaluated in rats by biodistribution studies and animal PET imaging studies.

Results: The radiolabeling reaction led to the desired [^{18}F]**1**. After HPLC purification no-carrier-added [^{18}F]**1** was obtained (radiochemical yield, 23−47% (n = 10,); radiochemical purity > 99%; molar activity, 15−28 GBq/μmol). Biodistribution studies with [^{18}F]**1** showed good brain uptake (1.04% dose/g at 2 min post-injection), high uptake into the hypothalamus (1.55% dose/g at 30 min), and a high target-to-non-target (hypothalamus to cerebellum) ratio of 6:10 at 120 min post-injection. A PET imaging study in normal rats showed excellent uptake in the midbrain and thalamus regions known to be rich in SERT binding sites at 60 min after iv injection. Chasing experiment with escitalopram (iv, 2 mg/kg) in a rat at 60 min after iv injection caused a noticeable reduction in the regional radioactivity and the target-to-non-target ratio, suggesting binding by [^{18}F]**1** was highly specific and reversible for SERT binding sites in the brain.

Conclusions: A novel diphenyl sulfide derivative, [^{18}F]**1** for SERT imaging was successfully prepared and evaluated. Results suggest that this new chemical entity is targeting SERT binding sites in the brain, and it is a suitable candidate for future commercial development.

Abbreviations: DASB, (*N*,*N*-dimethyl-2-(2-amino-4-cyanophenylthio)benzyl-amine; (+)-McN5652, trans-1,2,3,5,6,10-<beta>-hexahydro-6-[4-(methylthio)phenyl-[pyrrolo-[2,1-<alpha>]isoquinoline; ADAM: 2-((2-((dimethylamino)methyl)-phenyl)thio)-5-iodo-phenylamine; 4-FADAM, (*N*,*N*-dimethyl-2-(2-amino-4-fluorophenylthio)benzylamine); IDAM, (5-iodo-2-((2-(dimethylaminomethyl)-phenylthio)benzylalcohol); FPBM, 2-(2'-((dimethylamino)methyl)-4'-(3-fluoropropoxy)phenyl-thio)benzenamine; 2-INXT, (R)-N-methyl-(2-iodo-phenoxy)-3-phenylpropylamine; IPT, N-(3-iodopropen-2-yl)-2beta-carbomethoxy-3beta-(4-chlorophenyl) tropane; LLC-PK1, Hampshire pig kidney cells; BSA, bovine serum albumin; GBR12909, 1-(2-[bis(4-fluorophenyl)methoxy]ethyl)-4-(3-phenylpropyl) piperazine; nisoxetine, (±)-N-methyl-3-(2′-methoxyphenoxy)-3-phenylpropylamine; PET, positron emission tomography; SPECT, single photon emission computed tomography; SERT, serotonin transporter; NET, norepinephrine transporter; DAT, dopamine transporter; SSRI, selective serotonin reuptake inhibitor; K_{222}, Kryptofix 222; DCM, dichloromethane; DMF, dimethylformamide; DMSO, dimethyl sulfoxide; EA, ethylacetate; MeCN, acetonitrile; THF, tetrahydrofuran.

1. Introduction

Serotonin is a major neurotransmitter that plays an important role in maintaining neuronal function in the central nervous system. Serotonin transporters (SERT) localized on presynaptic serotonin neurons serve as the main re-uptake mechanism for terminating the action of serotonin by transporting serotonin, the neurotransmitter, from the synaptic cleft back into the presynaptic neuron. These transporters play a very important role in controlling the serotonin concentration in the synapse and its binding to the postsynaptic serotonin receptors. Selective serotonin reuptake inhibitors, SSRIs, such as fluoxetine, sertraline, paroxetine, and escitalopram, specifically target SERT and prevent serotonin reuptake to the neurons. Consequently, SSRIs are useful in the treatment of depression as well as many other psychiatric conditions by controlling the concentration of serotonin in the synapse [1]. SSRIs are generally prescribed as the first-line therapy for depression and are some of the most commonly used drugs in the world [2]. Positron emission tomography (PET) imaging with suitably ^{18}F-labeled SERT inhibitors or ^{123}I-labeled diphenyl sulfides for single photon emission tomography (SPECT) may be useful as a method for probing pathophysiological and therapeutic mechanisms in various psychological diseases [3]. A number of SERT ligands for in vivo imaging (Fig. 1) have been developed [4-14]. [^{11}C]McN5652 was the first SERT PET imaging tracer used in humans. However, use of this tracer is limited due to high nonspecific binding, slow uptake kinetics in SERT-rich brain regions [12, 15, 16], and the short half-life of carbon-11. Development of the [^{18}F]FMe-(+)-McN5652, S-[^{18}F]fluoromethyl analogue of (+)-McN5652 showed favorable features for SERT imaging with PET in humans [12]. It is also suitable for in vivo quantification of SERT with PET.

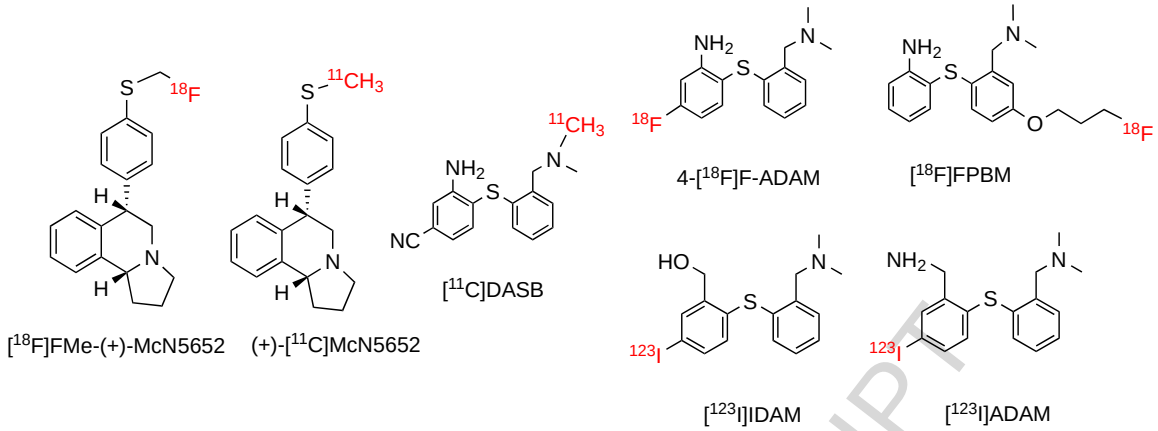

Fig. 1. Chemical structures of selected positron emission tomography (PET, labeled with fluorine-18 and carbon-11) and single photon emission tomography (SPECT, labeled with iodine-123) imaging agents for serotonin transporters (SERT). The most commonly used SERT imaging agents are diphenyl sulfides, including DASB, ADAM, IDAM, and FPBM shown above.

Ligands containing a core structure of diphenyl sulfide showed promising results as in vivo SERT imaging agents (Fig. 1) [17, 18]. Previously, one diphenyl sulfide tracer, [^{123}I]ADAM, has been evaluated in humans and demonstrated feasibility for SPECT imaging of SERT in the brain [19]. The most commonly used PET imaging agent for SERT is [^{11}C]DASB [20, 21]. It exhibits excellent selectivity, high reproducibility, and simple kinetic modeling for quantification [22, 23]. Recent reports suggest that altered SERT availability can be measured in social anxiety disorder [24] and obsessive-compulsive disorder [25] by [^{11}C]DASB/PET. However, [^{11}C]DASB is a ^{11}C-labeled radiotracer that is limited by its short physical half-life (20 min), which is unsuitable for widespread clinical application. Fluorine-18 has a longer half-life (110 min) and can be produced in several Bq of activity using a cyclotron. The longer half-life makes it feasible to prepare the ^{18}F-radiolabeled agent at radiopharmacies and distribute the PET imaging agent regionally, thus making it available to many hospitals. Significant efforts have been made to develop such ^{18}F-labeled radiotracers for SERT imaging [11, 17, 26, 27]. One promising ^{18}F-labeled ligand is 4-[^{18}F]FADAM [28] (Fig. 1). Results from the first human study of 4-[^{18}F]FADAM [14] showed that it is safe and effective for mapping SERT regional binding sites in the brain. The regional specific uptake in the human brain

correlated well with the known distribution of SERT. The optimal imaging time (about 120 min) was slightly long, but acceptable for routine clinical use. The major drawback of 4-[^{18}F]FADAM is associated with its low labeling yields (1−5%), which limits its widespread clinical application [29].

An alternative diphenyl sulfide derivative, [^{18}F]FPBM (Fig. 2) with a different substitution on the phenyl ring, has been shown to possess high selective binding (K_i = 0.38 nM), brain uptake (0.99% dose/g at 2 min after IV injection), and an excellent in vivo target-to-non-target ratio (7.7 at 120 min post-injection) [6, 30, 31]. Previously, the labeling of this diphenyl sulfide was performed using a nucleophilic fluorination with [^{18}F]F$^-$/$K_{2.2.2}$ via TsO-precursor [32, 33]. The desired product, [^{18}F]FPBM, was further purified using either high-performance liquid chromatography (HPLC) or solid phase extraction (SPE), resulting in useful radiochemical yields (24−33%) [32]. However, [^{18}F]FPBM does not have patent protection; therefore, it is not a candidate for commercial development. A new chemical entity is needed for future development of a commercial product for PET imaging of SERT in the brain.

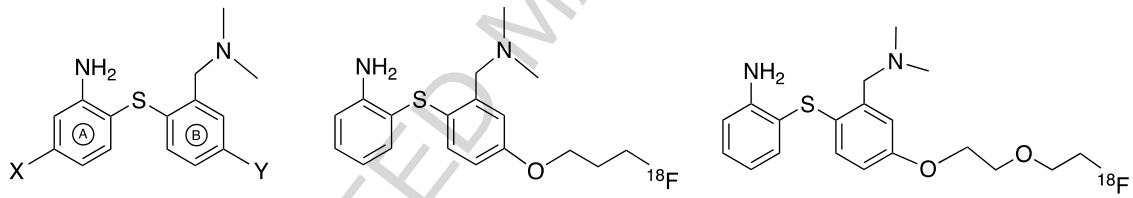

core structure of ADAM/DASB/ FPBM and derivatives [^{18}F]FPBM [^{18}F]**1**

Fig. 2. Core structures of ADAM/DASB/FPBM and chemical structures of [^{18}F]FPBM and [^{18}F]**1**

As part of an effort to systematically investigate and develop new compounds for commercial development, we have prepared several new derivatives of FPBM. We have modified the substitution for the 4′-(fluoroalkoxy) group on the B ring (Fig. 2). These are new derivatives of FPBM that showed interesting high bulk tolerance and retained the desired SERT binding affinity. The new SERT ligands were prepared using the reactions described in Scheme 1. The goal of this effort was to test the brain uptake and selectivity of regional binding for SERT binding sites in the hypothalamus (midbrain) area. The improvement may serve as the basis for a PET imaging agent in determining the SERT

binding in the brain. Reported herein are the syntheses of four different novel diphenyl sulfide derivatives, **1**−**4.** Among them, compound **1** was chosen for further radiolabeling and biological evaluation (Scheme 1). This new ligand may be suitable for future development as a commercial product for PET imaging of SERT in the brain.

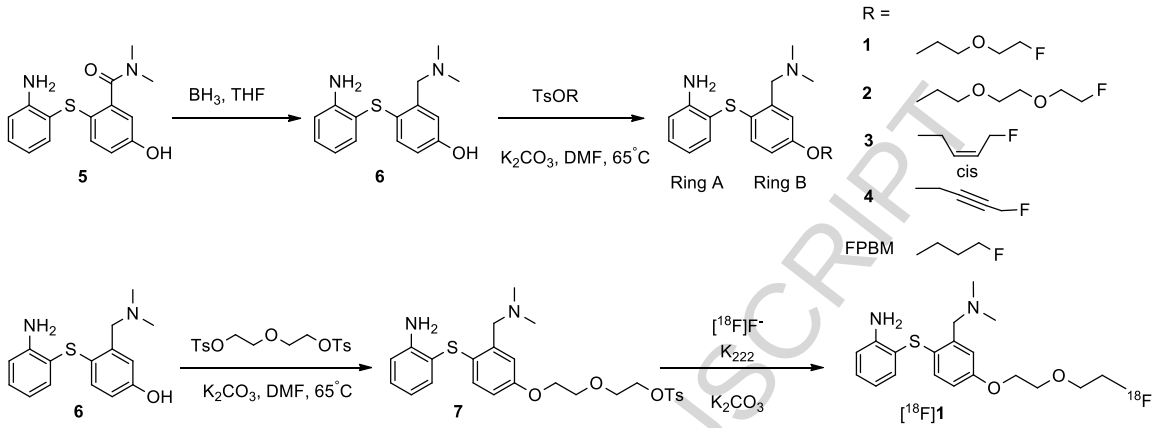

Scheme 1. Preparation of compounds **1**−**4** and the -OTs precursor **7** for ^{18}F radiolabeling. Several precursors of TsOR substituted groups were readily prepared according to the literature [34].

2. Materials and Methods

All the reagents and solvents were commercial products and were used without further purification unless otherwise indicated. Solid-phase extraction cartridges (Oasis HLB 3cc cartridge, QMA light cartridge) were obtained from Waters (Milford, MA, USA). Thin-layer chromatography (TLC) was run on pre-coated plates of silica gel 60 F254. ^{1}H and ^{13}C nuclear magnetic resonance (NMR) spectra were recorded on a Bruker AVANCE II 400 spectrometer and are reported in parts per million (ppm) from the residual solvent peak ($CDCl_3$). High-resolution mass spectrometry was measured using Agilent (liquid chromatography/mass selective detector with time of flight) mass spectrometry. High-performance liquid chromatography was performed on an Agilent 1200 series system with a reversed phase column (C18 reversed phase, Phenomenex and Agilent). ^{18}F aqueous solution was provided by Peking University Cancer Hospital.

Male Sprague Dawley rats (190−220 g) were purchased from Beijing Vital River Laboratory Animal Technology Co., Ltd. All the procedures of the animal experiments were performed in compliance with relevant laws and institutional guidelines. All the

animal protocols were approved by the Institutional Animal Care and Use Committee of Beijing Normal University and the University of Pennsylvania.

2.1. Chemical synthesis

2.1.1. *4-((2-aminophenyl)thio)-3-((dimethylamino)methyl)phenol* (**6**)

BH_3 in THF (1 mol/L, 3.47 mL,) was added dropwise at room temperature to a mixture of 2-((2-aminophenyl)thio)-5-hydroxy-*N*,*N*-dimethylbenzamide (**5**) [32](200 mg, 0.69 mmol) in anhydrous THF (4 mL). The reaction mixture was refluxed for 8 h and cooled with an ice bath. Concentrated HCl (0.5 mL) was cautiously added and the solvent was removed from the vacuum. HCl solution (1 mol/L, 10 mL) was then added and refluxed for 1 h. The reaction mixture was cooled to room temperature and adjusted to pH = 9 with a saturated solution of Na_2CO_3 and extracted with ethyl acetate (20 mL × 3). The organic layers were combined and dried over anhydrous $MgSO_4$ and filtered. The filtrate was evaporated in a vacuum and purified by flash chromatography (silica gel) (methanol/EA, 0% to 10%, v/v) to obtain 4-((2-aminophenyl)thio)-3-((dimethylamino)methyl)phenol (**6**) (135 mg, yield: 71%) as a colorless viscous oil. ^{1}H NMR (400 MHz, $CDCl_3$) δ 7.31 (dd, J = 7.6, 1.3 Hz, 1H), 7.19−7.13 (m, 1H), 6.88 (d, J = 8.5 Hz, 1H), 6.79−6.67 (m, 3H), 6.57 (dd, J = 8.5, 2.8 Hz, 1H), 3.59 (s, 2H), 2.33 (s, 6H). ^{13}C NMR (100 MHz, $CDCl_3$) δ 155.27, 147.86, 138.43, 135.77, 131.29, 129.91, 125.96, 118.58, 117.92, 117.45, 116.15, 115.40, 61.46, 45.11. HRMS calcd. for $C_{15}H_{18}N_2OS$ $[M+H]^+$ 275.1218. Found 275.1163.

2.1.2. *General procedure A for the preparation of **1**−**4***

A mixture of 4-((2-aminophenyl)thio)-3-((dimethylamino)methyl)phenol **(6)** (0.2 mmol) and K_2CO_3 (83 mg, 0.6 mmol) was stirred in anhydrous DMF (3 mL) at 65 °C for 1.5 h. The TsOR substituted groups were prepared according to the literature [34]. Compound TsOR (0.3 mmol) was added and the mixture was stirred for another 2 h and then cooled to room temperature. Saturated solution of NaCl (12 mL) was added and the reaction mixture was extracted with ethyl acetate (15 mL × 3). The organic layers were combined and dried over $MgSO_4$ and filtered. The filtrate was evaporated in a vacuum and purified by flash chromatography (silica gel) (methanol/DCM, 0% to 10%, v/v) to obtain **1**−**4** as a colorless viscous oil.

2-((2-((dimethylamino)methyl)-4-(2-(2-fluoroethoxy)ethoxy)phenyl)thio)aniline (**1**) was prepared using 4-((2-aminophenyl)thio)-3-((dimethylamino)methyl)phenol (**6**), 2-(2-fluoroethoxy)ethyl-4-methylbenzenesulfonate, and procedure A to obtain product **1** as a colorless viscous oil at a yield of 40%. ^{1}H NMR (400 MHz, $CDCl_3$) δ 7.41 (dd, J = 8.0, 1.5 Hz, 1H), 7.19−7.15 (m, 1H), 6.95 (d, J = 8.6 Hz, 1H), 6.92 (d, J = 2.8 Hz, 1H), 6.75−6.68 (m, 3H), 4.69−4.63 (m, 1H), 4.59−4.50 (m, 1H), 4.17−4.08 (m, 2H), 3.89−3.85 (m, 3H), 3.80−3.75 (m, 1H), 3.56 (s, 2H), 2.31 (s, 6H).^{13}C NMR (100 MHz, $CDCl_3$) δ 157.22, 148.34, 139.20, 136.41, 130.66, 130.12, 127.45, 118.18, 117.02, 116.65, 115.23, 114.19, 84.01, 82.33, 70.69, 70.49, 69.92, 67.54, 62.41, 45.34. HRMS calcd. for $C_{19}H_{25}FN_2O_2S$ $[M+H]^+$ 365.1699. Found 365.1704.

2-((2-((dimethylamino)methyl)-4-(2-(2-(2-fluoroethoxy)ethoxy)ethoxy)phenyl)thio)aniline (**2**) was prepared using 4-((2-aminophenyl)thio)-3-((dimethylamino)methyl)phenol (**6**), 2-(2-(2-fluoroethoxy)ethoxy)ethyl 4-methylbenzenesulfonate, and procedure A to obtain product **2** as a colorless viscous oil at a yield of 41%.^{1}H NMR (400 MHz, DMSO) δ 7.25−7.06 (m, 3H), 6.93 (s, 2H), 6.75 (d, J = 7.6 Hz, 1H), 6.55 (t, J = 7.2 Hz, 1H), 4.59−4.52 (m, 1H), 4.47−4.41 (m, 1H), 4.08 (s, 2H), 3.87−3.34 (m, 10H), 2.46 (s, 6H). HRMS calcd. for $C_{21}H_{29}FN_2O_3S$ $[M+H]^+$ 409.1961. Found 409.1494.

(Z)-2-((2-((dimethylamino)methyl)-4-((4-fluorobut-2-en-1-yl)oxy)phenyl)thio) aniline (**3**) was prepared using 4-((2-aminophenyl)thio)-3-((dimethylamino)meth yl)phenol(**6**), (Z)-4-fluorobut-2-en-1-yl 4-methylbenzene-sulfonate, and procedure A to obtain product **3** as a colorless viscous oil at a yield of 36%.^{1}H NMR (400 MHz, DMSO) δ 7.38−7.06 (m, 3H), 6.98−6.92 (m, 2H), 6.78 (d, J = 8.0 Hz, 1H), 6.55 (dd, J = 10.7, 4.1 Hz, 1H), 5.94−5.80 (m, 2H), 5.15 (d, J = 4.3 Hz, 1H), 5.04 (d, J = 5.6 Hz, 1H), 4.69 (s, 2H), 4.37 (s, 2H), 2.68 (s, 6H). HRMS calcd. for $C_{19}H_{23}FN_2OS$ $[M+H]^+$ 347.1593. Found 347.1361.

2-((2-((dimethylamino)methyl)-4-((4-fluorobut-2-yn-1-yl)oxy)phenyl)thio)aniline (**4**) was prepared using 4-((2-aminophenyl)thio)-3-((dimethylamino)methyl)phenol(**6**), 4-fluorobut-2-yn-1-yl 4-methylbenzenesulfonate and procedure A to obtain product **4** as a

colorless viscous oil at a yield of 37%.^{1}H NMR (400 MHz, DMSO) δ 7.22 (dd, J = 7.6, 1.2 Hz, 1H), 7.16−7.05 (m, 2H), 6.87 (s, 2H), 6.74 (d, J = 7.9 Hz, 1H), 6.57−6.53 (m, 1H), 5.20 (s, 1H), 5.08 (s, 1H), 4.91 (d, J = 7.5 Hz, 2H), 3.79 (s, 2H), 2.38 (s, 6H). HRMS calcd. For $C_{19}H_{21}FN_2OS$ $[M+H]^+$ 345.1437. Found 345.1211.

2.1.3. *2-(2-(4-((2-aminophenyl)thio)-3-((dimethylamino)methyl)phenoxy)ethoxy)ethyl 4-methylbenzenesulfonate* (**7**)

A mixture of 4-((2-aminophenyl)thio)-3-((dimethylamino)methyl)phenol (**6**) (60 mg, 0.22 mmol) and K_2CO_3 (91 mg, 0.66 mmol) was stirred in anhydrous DMF (3 mL) at 65 °C for 1.5 h. Oxybis(ethane-2,1-diyl) bis(4-methylbenzenesulfonate) (136 mg, 0.33 mmol) was then added and the mixture was stirred for another 2 h and cooled to room temperature. Saturated solution of NaCl (12 mL) was added and the reaction mixture was extracted with ethyl acetate (15 mL × 3). The organic layers were combined and dried over $MgSO_4$ and filtered. The filtrate was evaporated in vacuum and purified by flash chromatography (silica gel) (methanol/DCM, 0% to 10%, v/v) to obtain 2-(2-(4-((2-aminophenyl)thio)-3-((dimethylamino)methyl)-phenoxy)ethoxy)ethyl 4-methylbenzenesulfonate (**7**) (60 mg, yield: 53%) as a colorless viscous oil. ^{1}H NMR (400 MHz, $CDCl_3$) δ 7.81 (d, J = 8.3 Hz, 2H), 7.41 (dd, J = 8.0, 1.4 Hz, 1H), 7.32 (d, J = 8.0 Hz, 2H), 7.20−7.14 (m, 1H), 6.95 (d, J = 8.6 Hz, 1H), 6.89 (d, J = 2.5 Hz, 1H), 6.75−6.64 (m, 3H), 4.55 (brs, 2H), 4.22−4.17 (m, 2H), 4.04−3.98 (m, 2H), 3.76 (dd, J = 9.3, 4.5 Hz, 4H), 3.56 (s, 2H), 2.43 (s, 3H), 2.31 (s, 6H).^{13}C NMR (100 MHz, $CDCl_3$) δ 157.22, 148.31, 144.81, 136.34, 132.97, 130.75, 130.15, 129.82, 127.99, 127.50, 125.93, 118.24, 116.95, 116.56, 115.26, 114.33, 69.85, 69.20, 68.89, 67.47, 62.20, 45.23, 21.62. HRMS calcd. for $C_{26}H_{32}N_2O_5S_2$ $[M+H]^+$ 517.1831. Found.517.1815.

2.2. Preparation of LLC-SERT, LLC-NET, and LLC-DAT membrane homogenates

Hampshire pig kidney (LLC-PK1) cells expressing the rat serotonin (SERT), human norepinephrine (NET) or rat dopamine transporter (DAT) were kindly provided by Dr. Gary Rudnick (Yale University) [35]. The parental LLC-PK1 cell line was derived from pig renal epithelial cells, which do not express SERT, NET, or DAT. Thus, the monoamine transport activity of LLC-SERT, LLC-NET, and LLC-DAT is due only to

the corresponding transfected DNA. The cells were cultured and grown to confluence as a monolayer with DMEM containing 10% FBS, 1 × penicillin/streptomycin, and 1 g/L G418. The cells were then washed with PBS containing 100 mg/mL calcium and 100 mg/mL magnesium (Gibco-Invitrogen), homogenized on ice with a Wheaton overhead stirrer, and centrifuged at 16,500 rpm for 20 min at 4 ºC. The supernatant was discarded, and the pellet was then suspended in PBS, quickly frozen in liquid nitrogen, and moved to a −80 ºC freezer for future use.

2.3. In vitro binding assays

All the binding assays were performed in glass tubes (12 × 75 mm) with a final volume of 0.2 mL. First, LLC-SERT/LLC-DAT/LLC-NET homogenates (100 μL, 30−60 μg protein) were mixed with 50 mM Tris-HCl, pH 7.4, 120 mM NaCl, and 5 mM KCl and 1 mg/mL bovine serum albumin (BSA) to overcome the stickiness. 0.1−0.2 nM of [^{125}I]IDAM (K_d = 0.09 nM), [^{125}I]IPT (K_d = 1.2 nM), and [^{125}I]INXT (K_d = 0.06 nM) were the characterized as the radioligands of choice [36]. Competition experiments were performed using [^{125}I]IDAM and a range of 10 concentrations (10^{-10} to 10^{-5} M) of the compounds to be evaluated. Competing compounds were serially diluted with buffer (as above) containing 0.1% BSA to overcome the stickiness and loss due to dilution. Non-specific binding was defined with 1 μM of citalopram HBr (TOCRIS Bioscience), GBR-12909, and nisoxetine (NIMH), corresponding to SERT, DAT, and NET, respectively. Incubation was carried out at room temperature for 60 min [6]. After the 60-minute incubation period, separation of the bound from free radioligands was conducted via filtration through glass fiber filters pre-soaked with 1% polyethylenimine (Sigma-Aldrich, St. Louis, MO, USA). The filters were then washed three times with ice cold 50 mM Tris-HCl (3 mL) and pH 7.4 buffer and counted in a gamma counter (Cobra II, PerkinElmer, Waltham, MA, USA) with 70% efficiency. The results of the experiments were determined using Microsoft Excel.

2.4. Radiolabeling chemistry of [^{18}F]1

[^{18}F]**1** was prepared using the one-step radiochemical reaction described in Scheme 1. [^{18}F]fluoride (740−1110 MBq), produced by a cyclotron using the ^{18}O(p,n)^{18}F

reaction, was trapped on a Sep-Pak Light QMA cartridge (preconditioned with 10 mL 0.5 mol/L $NaHCO_3$ solution and 10 mL water). The ^{18}F-activity was eluted with phase transfer catalyst solution (11.0 mg Kryptofix222 and 2.0 mg K_2CO_3 in 0.93 mL acetonitrile and 0.17 mL water). The eluate was added into a 10 mL test tube and evaporated at 90 °C under a stream of N_2. The residue was azeotropically dried twice with anhydrous acetonitrile (2 mL) at 90 °C under a stream of N_2. The precursor, **7**, was dissolved in anhydrous acetonitrile (1 mL). The precursor solution was added to a test tube containing the dried residue prepared above. The mixture was then vortexed, sealed and heated at 90 °C for 10 min. The reaction mixture was quenched in ice water, and water (10 mL) was added. The mixture was passed through an Oasis HLB 3 cc cartridge (preconditioned with 10 mL ethanol and 10 mL water). The cartridge was washed with water (10 mL) and 10% ethanol/H_2O (v/v, 5 mL). The desired product was eluted from the cartridge with acetonitrile (1.5 mL) and purified using a semi-prep HPLC system. The HPLC was equipped with a gamma ray radio detector and a UV/Vis detector [Agilent XDB-C18 column (9.4 × 250 mm, 5 μm), mobile phase: 55% 20 mM ammonium formate buffer and 45% acetonitrile, 3 mL/min, 254 nm. Retention time: [^{18}F]**1** = 9−11 min].

The mobile phase containing [^{18}F]**1** was collected and diluted with water (20 mL). The solution was passed through an Oasis HLB 3 cc cartridge (preconditioned with 10 mL ethanol and 10 mL water). [^{18}F]**1** was trapped on the cartridge and washed with water (10 mL). The final product was eluted from the cartridge with ethanol (10 mL).

Chemical identification of the purified product was carried out by HPLC co-injection with compound **1** using a UV/Vis detector at 254 nm and a gamma ray radio detector. Two HPLC conditions were used: (1) Phenomenex Gemini C18 column (150 × 4.6 mm, 5 μm). Mobile phase: 1 mL/min with a gradient as follows: from 0 to 3 min, isocratic 10 mM ammonium formate buffer (AFB) 98% and MeCN 2%; from 3 to 5 min, gradient AFB 98−50%, MeCN 2−50%; from 5 to 10 min, gradient AFB 50−0%, MeCN 50−100%; from 10 to 17.5 min, gradient AFB 0−98%, MeCN 100−2%; from 17.5 to 20 min, isocratic AFB 98% and MeCN 2%. Retention time: [^{18}F]**1** = 12.0−13.0 min, [^{18}F]fluoride = 1.5−2.0 min. (2) Supelco Ascentis C18 (150 × 4.6 mm, 5 μm) MeCN/10 mM AFB 40/60, 1 mL/min. (The radiochemical purity (RCP) was measured by TLC analysis [pre-coated silica gel, 60 F254 plates with

dichloromethane/methanol/triethylamine = 10/1.1/0.35 v/v/v] and HPLC. At the end of the synthesis, the radiochemical yield was 23−47% (n = 10,) with a radiochemical purity of > 99% and a molar activity of 15−28 GBq/μmol (Fig. 3). The final product was dried under a stream of nitrogen, then re-dissolved in ethanol (100 μL) and diluted with saline.

2.5. Determination of log D value

To measure the partition coefficient, 3 mL of 1-octanol and 3 mL of 0.1 M NaH_2PO_4 buffer (pH 7.4) were added to roughly 1 million cpm of [^{18}F]**1** dissolved in < 10 μL of ethanol and vortexed for 1 min. The mixture was then centrifuged for 3 min. Samples of 2 mL each of the 1-octanol and buffer layers were weighed and then counted in a gamma counter. Additional 1-octanol was added to increase the 1-octanol fraction sample to 3 mL, and an additional 3 mL of buffer was then added. The mixture was vortexed and centrifuged again as above. This procedure was repeated 3 times. The partition coefficient was determined by calculating the ratio of cpm/mL of 1-octanol to that of the buffer after the third partition.

2.6. Biodistribution in rats

Five rats per group were used for each biodistribution study. While under isoflurane anesthesia, saline solution (0.2 mL, ethanol < 5% total volume) containing 1.48−2.59 MBq of the radioactive tracer [^{18}F]**1** (0.0099−0.017 nmol carrier)was injected into the femoral vein. The rats were sacrificed at the indicated times (2, 30, 60, and 120 min) while under isoflurane anesthesia. The organs of interest were removed and weighed, and the radioactivity was counted. The percent dose per organ was calculated by comparing the tissue counts to counts of 1% of the initial dose (100 times diluted aliquots of the injected material) measured at the same time. Regional brain distribution in the rats was measured after an IV injection of the radioactive tracer. Samples from different brain regions (cortex, striatum, cerebellum, and hypothalamus) were dissected, weighed, and counted. The percentage dose/g of each sample was calculated by comparing the sample counts to the counts of the diluted initial dose described above. The ratio was calculated by dividing the percentage dose/g of each region by that of the cerebellum. The cerebellum was used as the reference region for calculating the ratio of

target to non-target binding, because only a trace amount of SERT is present in the cerebellum.

2.7. In vivo blocking studies

A SERT and NET selective inhibitor (2 mg/kg escitalopram, 10 mg/kg nisoxetine, respectively) was injected into the rat by the femoral vein with [^{18}F]**1** (1.48−2.59 MBq) simultaneously. Regional brain distribution, as in the biodistribution studies described above, was determined 120 min after injection of the radioactive tracer.

2.8. In vivo metabolism of [^{18}F]1

Rats were anesthetized with 1.5% isoflurane. The animals were injected with 37–74 MBq of [^{18}F]**1** (0.2 mL, 10% ethanol in saline). The animals were then sacrificed at 5 or 120 min after the intravenous injection. Blood and brain were harvested. Blood samples were centrifuged at 15,000 g for 5 min at 4 °C to separate plasma from the clot. Plasma was then collected and the same volume of MeCN was added and the mixture was vortexed and centrifuged at 15,000 g for 5 min for deproteinization. Brain was homogenized in a solution of three volumes of MeCN. Homogenates were then centrifuged at 15,000 g for 5 min at 4 °C and the supernatant was collected. An aliquot of the supernatant obtained from plasma and brain homogenate was injected into the radio-HPLC system, and analyzed under the analytical conditions described above. The percentages of [^{18}F]**1** relative to total radioactivity on HPLC were calculated as (peak area for unchanged tracer peak / total peak area) × 100.

2.9. PET Imaging in rats

The radiotracer was dissolved in a small volume of saline solution (ethanol < 5% total volume). Approximately 40.7−55.5 MBq of the radiotracer (0.27−0.37 nmol carrier, 200−300 μL)was injected through the tail vein. Imaging was performed using the Philips Mosaic Animal PET (A-PET) imaging system, which has an image field of view of ~11.5 cm. Data acquisition commenced at the time of [^{18}F]**1** injection. Scans were carried out over a period of 2 h at 5 min per frame. The image voxel size was 0.5 mm^3.

Region-of-interest analysis was performed using AMIDE [37] on reconstructed images. To examine the specificity of [^{18}F]**1** for SERT, an injection of escitalopram (2 mg/kg) was delivered 60 min after [^{18}F]**1** injection.

3. Results

3.1. In vitro binding assays

The binding affinity of nonradioactive diphenyl sulfides, **1**−**4**, was evaluated using stably transfected LLC-PK$_1$ cell lines overexpressing SERT, NET, and DAT (Table 1). Compounds **1**−**3** displayed excellent binding affinity to SERT ($K_{i,\ SERT}$ = 0.09, 0.22, and 0.02 nM, respectively) and selectivity over DAT ($K_{i,\ DAT}$ = 370, 586, and 686 nM, respectively). DAT and NET affinities were not evaluated for compound **4** as it showed lower affinity to SERT. Compounds **1**−**3** also displayed binding affinity for NET affinities, but NET/SERT selectivity was > 10 and the selectivity would be acceptable. Among these new SERT binding agents, we have selected **1** for radiolabeling and further biological evaluation. Attempts at radiolabeling new agents **2**−**4**, were unsuccessful and further evaluation was carried out.

3.2. Biodistribution

In order to evaluate the organ and regional brain biodistribution in the rats, [^{18}F]**1** was injected through the femoral vein, and after selected time points, the rats were sacrificed. [^{18}F]**1** showed a relatively high brain uptake at 2 min post-injection (brain uptakes at 2, 30, 60, and 120 min were 1.04, 0.91, 0.86, and 0.67% dose/g, respectively; Table 2).

Regions of rat brain were dissected and counted to determine whether regional brain uptake and retention of [^{18}F]**1** was consistent with the regional density of SERT. The results showed the highest uptake in the hypothalamus, a SERT-rich region, as well as uptake in the lower SERT-containing regions, striatum, and cortex. The cerebellum, known to have a low SERT concentration, was used as the background region for calculating the target-to-non-target binding ratio. The distribution result of [^{18}F]**1** was similar to [^{18}F]FPBM; at 120 min after IV injection, the uptake in the hypothalamus region was 1.2 and 0.76% dose/g, respectively, and the hypothalamus/cerebellum ratio

was 6.1 and 7.6, respectively. The results indicated that [^{18}F]**1** showed very good in vivo brain kinetic property, useful for imaging similar to that of [^{18}F]FPBM [6, 30, 31].

3.3 In vivo blocking studies

Co-injection with selective monoamine transporter inhibitors demonstrated the SERT selectivity of [^{18}F]1 in vivo in rats (Table 3 and Fig. 4A). A 120 min time point was chosen for these pharmacological blocking biodistribution studies. Co-injection with escitalopram, a selective SERT inhibitor, greatly reduced regional brain uptake (1.17 to 0.40% dose/g for the hypothalamus, similar to [^{18}F]FPBM, Fig. 4B) and target-to-nontarget ratios (6.54 to 2.09 for hypothalamus to cerebellum, Table 3) when compared to control. While Co-injection with nisoxetine (NET selective inhibitor) showed only tiny inhibition.

3.4. PET Imaging

Animal PET imaging of the rats' brains showed a good [^{18}F]**1** localization in the thalamus, midbrain, and striatum (Fig. 5). Typical nonspecific binding in the Harderian glands was also observed. As predicted, there was minimal uptake in the cerebellum, which was used as the background region for calculating target-to-non-target ratio. For image analysis, regions of interest (ROIs) (midbrain and striatum) were manually drawn to encompass only areas where high radioactivity was observable. The time activity curves (TACs) generated for the midbrain and striatum regions showed that [^{18}F]**1** uptake peaked at approximately 10 min (Fig. 6A) and steadily declined afterward. The region-to-cerebellum ratios peaked at about 90 min (Fig. 6B) and remained steady afterward. In a separate experiment, a rat was injected with [^{18}F]**1**, followed by an IV injection of 2 mg/kg escitalopram at 60 min. A fast reduction of activity in the midbrain and striatum was observed (Fig. 6C). A clear reduction in the midbrain to cerebellum ratio was observed, suggesting that they are competing for the same SERT binding sites in the brain (Fig. 6D).

4. Discussion

Imaging serotonin transporter (SERT) in the brain has been performed for the past 20 years. The high level of interest is a reflection of the importance of this transporter in regulation brain function in both normal and disease states. It was reported previously that [^{18}F]FPBM with fluoropropoxyl substitution on the B phenyl ring showed high selective binding (K_i = 0.38 nM), high brain uptake (0.99% dose/g at 2 min after IV injection), and an excellent in vivo target-to-non-target ratio (7.7 at 120 min post-injection) [6, 30, 31]. [^{18}F]FPBM was first reported 10 years ago, although the pre-clinical evaluations clearly suggested that it was an excellent candidate for SERT imaging in conjunction with PET. However, there is no patent protection filed for this agent, which limits its ability to attract new funding for commercial development. It is necessary to continue to develop additional derivatives, which are new chemicals. We have further modified the structure and tested several new compounds as potential SERT imaging agents with patent protection for commercial development.

In this report, the corresponding 2-(2-fluoroethoxy)ethoxy derivative, **1**, also exhibited an excellent binding affinity (K_i = 0.09 nM) for SERT. The new probe, [^{18}F]**1**, can be readily prepared via a simple one-step SN2 fluorination reaction. The partition coefficient was measured as log$D$ = 2.40 ± 0.05 (n = 3, pH 7.4), which is comparable to [^{18}F]FPBM (log$D$ = 2.54, pH 7.4).[30]. It also displayed excellent initial brain uptake (1.04% dose/g at 2 min post iv injection) and an excellent in vivo target-to-non-target ratio (6.1 at 120 min post-injection). High initial brain uptake at 2 min after iv injection suggests that the new SERT probe [^{18}F]**1** may lead to a high initial delivery into the brain tissue. Excellent washout from non-target region leads to a good target-to-non-target ratio (midbrain/cerebellum ratio). These results lend support to improve SERT target imaging in the brain. It is noted that previously in vivo brain metabolism of ^{123}I labeled diphenyl sulfide derivatives, IDAM and ADAM (Fig. 1), after iv injection has been investigated and found that at 60 and 120 min after the injection > 95% of the radioactivity in the brain was associated with the original compound [36, 38]. In an in vivo metabolism study, it was found that 96% of the radioactivity in the brain was still the parent ligand at 5 min after iv injection. Because of lower activity, we didn't investigate the metabolism at 120 min. We expect this series of similar diphenyl sulfide derivatives will show similar in

vivo metabolic properties in the brain; therefore, little or no in vivo metabolism is expected in the brain for [^{18}F]**1**.

Micro-PET imaging after iv injection of [^{18}F]**1** displayed excellent brain images that are consistent with the distribution of SERT density in the rat. An in vivo chasing experiment with injection of escitalopram (a commonly prescribed SERT targeting drug) exhibited a very good washout from the midbrain region, which further confirmed that this new probe competed for the same SERT binding sites in the brain. The results of this "chasing" experiment may be further supported in the future by performing pre-injection of the competing SERT inhibitor, such as escitalopram, for demonstrating the in vivo competition for the same SERT binding sites in the brain. Competition studies by coinjection of escitalopram (a known SERT specific ligand) with [^{18}F]1 in rats showed a reduction of ~60% in the SERT rich areas (striatum, cortex, hippocampus) at 120 min. postinjection suggesting specific activity.

It appears that the 2-(2-fluoroethoxy)ethoxy, which is a diglycol substitution group specifically on the B ring (Fig. 2), may increase the washout of the non-specific regions, leading to an excellent target-to-non-target ratio of the midbrain region, where SERT binding sites are highly concentrated. However, this observation needs to be confirmed by performing PET imaging in the human brain.

5. Conclusions

A new diphenyl sulfide derivative, 2-((2-((dimethylamino)-methyl)-4-(2-(2-[^{18}F]fluoroethoxy)ethoxy)phenyl)thio)aniline, [^{18}F]**1**, was prepared and evaluated for SERT binding. It showed excellent initial brain uptake, binding selectivity, and specific in vivo regional brain distribution matching SERT binding sites. This new PET tracer may be useful for studying SERT distribution in the human brain.

Acknowledgments

This work was financially supported in part by the Beijing Science and Technology Project (Z151100003915116) and the National Key Research and Development Program of China (2016YFC1306300).

The new recommendations on nomenclature were used in this manuscript [39].

Figure Legends

Fig. 1. Chemical structures of selected PET and SPECT imaging agents for serotonin transporters (SERT).

Fig. 2. Fig. 2. Core structures of ADAM/DASB/FPBM and chemical structures of [^{18}F]FPBM and [^{18}F]**1**

Fig. 3. HPLC profiles of **1** (**A**), [^{18}F]**1 (radiotrace)** (**B**)**,** and accompanying UV trace (**C**) (HPLC method 2).

Fig. 4. (A) The effects of NET (nisoxetine) and SERT (escitalopram) inhibitors for [^{18}F]**1** on regional brain distribution in normal rats (at 120 min, average of n = 5), Escitalopram inhibits uptake into the hypothalamus, striatum, cortex and hippocampus. (B) The effects of NET (nisoxetine) and SERT (IDAM) inhibitors for [^{18}F]FPBM on regional brain distribution in normal rats (at 120 min, average of n = 6), IDAM inhibits uptake into the hypothalamus, striatum, cortex and hippocampus.

* The data for [^{18}F]FPBM is reported previously[6].

Fig. 5. While under isoflurane anesthesia, 55.5 MBq of [^{18}F]**1** was injected through a catheter placed into the tail veins of the rats and scanning commenced. A-PET images (coronal, transverse, and sagittal views shown) of [^{18}F]**1** localization in the rat brains reflect known areas of SERT distribution. Total scan time was 2 h. One time frame is shown (0 to 60 min). [^{18}F]**1** localized in the midbrain (MB), cortex (CX), and thalamus (T), which are regions where SERT binding sites are concentrated. Activity due to nonspecific binding was detected in the Harderian glands (HG); this nonspecific binding is commonly observed in rats and mice for other PET agents. Little uptake is observed in the cerebellum (CB), a region with low SERT density.

Fig. 6. Kinetic data of [^{18}F]**1** after injection into a rat. **A**: Activity of [^{18}F]**1** (55.5 MBq injection) in the striatum (ST), midbrain (MB), and cerebellum (CB) over time. **B**: Ratio of ST/CB and MB/CB over time. **C**: Activity of [^{18}F]**1** (40.7 MBq injection) in ST, MB, and CB over time. After 60 min, escitalopram (2 mg/kg) was injected into the rat. **D**: Ratio of ST/CB and MB/CB over time with escitalopram (2 mg/kg) IV injection after 60 min. Data were generated from A-PET image analysis using AMIDE software. Values on the y-axis for graphs **A** and **C** are mean counts/voxel. **A**: After a 55.5 MBq injection of [^{18}F]**1**, the uptake peaked at 10 min and the activity counts in the non-target region, the

cerebellum, rapidly decreased. **B**: The regions (of interest)-to-cerebellum ratio peaked at approximately 100 to 110 min after IV injection. **C**: Intravenous injection of escitalopram (2 mg/kg) 60 min after a 40.7 MBq injection of [^{18}F]**1** (indicated by blue arrow) shows clear competition for SERT binding sites. Radioactivity in the target regions (ST and MB) decreased rapidly after escitalopram injection and reached cerebellar activity levels by 150 min. **D**: A dramatic decrease in the regions (of interest)-to-cerebellum ratio was also observed.

Scheme 1. The preparation of compounds **1**−**4** and the precursor **7** for ^{18}F radiolabeling.

Table 1. Binding affinities of compounds **1**−**4** to SERT, DAT, and NET (average of n = 3, K_i ± SD, nM)

Table 2. Biodistribution of [^{18}F]**1** in male SD rats (average of n = 5, % dose/g ± SD)

Table 3. The effects of SERT and NET inhibitors on region-to-cerebellum ratios (at 120 min, average of n = 5): Escitalopram greatly decreased the region-to-cerebellum ratio and little to no inhibition was seen with nisoxetine.

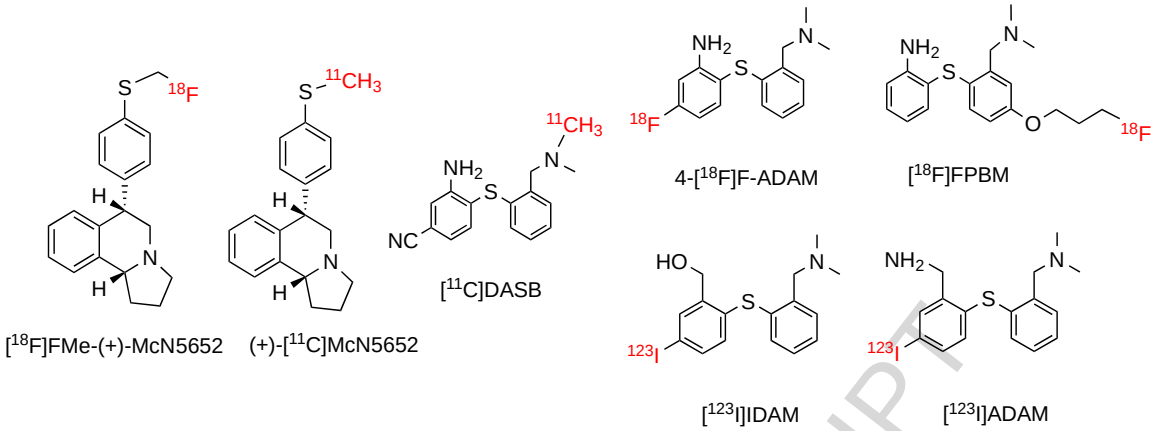

Fig. 1. Chemical structures of selected PET and SPECT imaging agents for serotonin transporters (SERT).

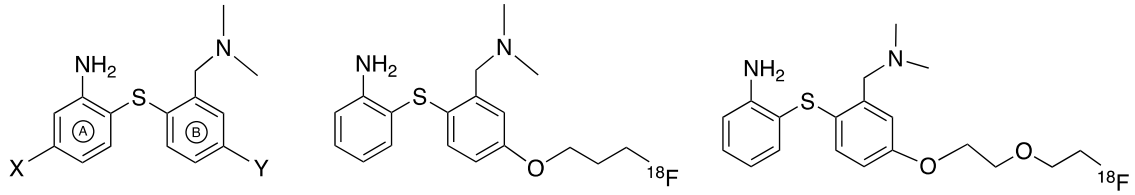

core structure of ADAM/DASB/ FPBM and derivatives

[^{18}F]FPBM

[^{18}F]**1**

Fig. 2. Core structures of ADAM/DASB/FPBM and chemical structures of [^{18}F]FPBM and [^{18}F]**1**

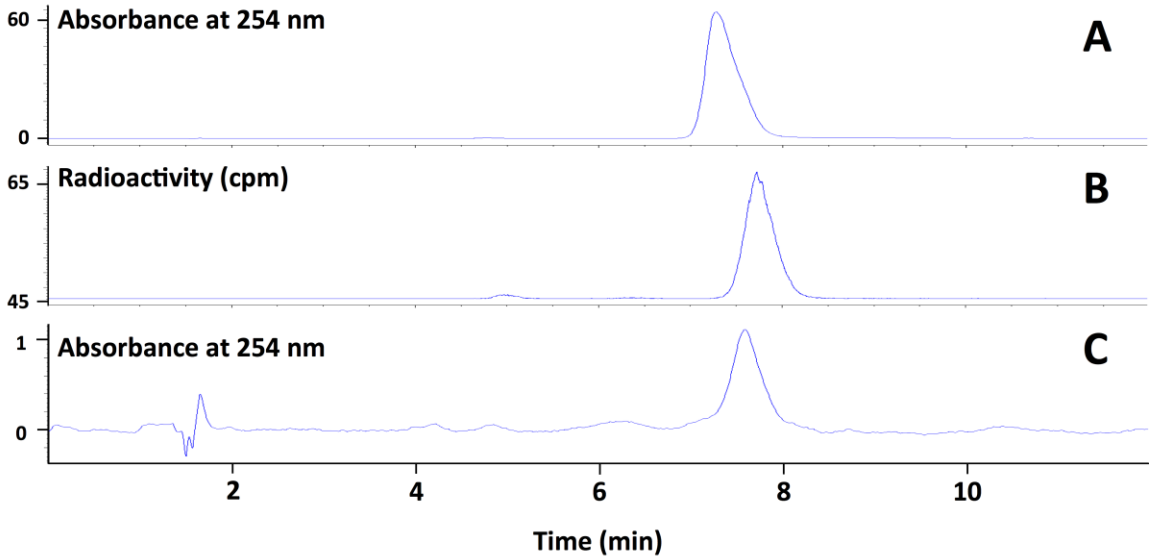

HPLC: Supelco Ascentis C18 (150 × 4.6 mm, 5 µm) ACN/10 mM AFB 40/60, 1 mL/min.

Fig. 3. HPLC profiles of **1** (**A**), [^{18}F]**1 (radiotrace)** (**B**)**,** and accompanying UV trace (**C**) (HPLC method 2).

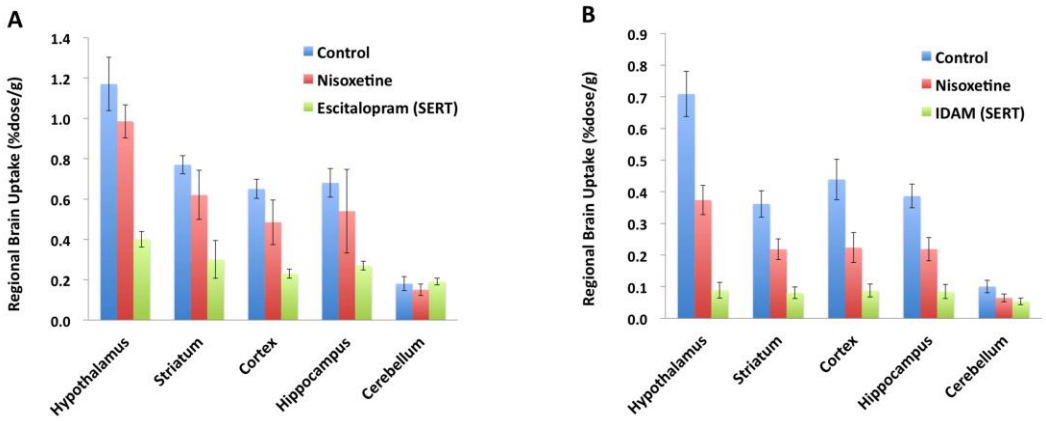

Fig.4. (A) The effects of NET (nisoxetine) and SERT (escitalopram) inhibitors for [^{18}F]**1** on regional brain distribution in normal rats (at 120 min, average of n = 5), Escitalopram inhibits uptake into the hypothalamus, striatum, cortex and hippocampus. (B) The effects of NET (nisoxetine) and SERT (IDAM) inhibitors for [^{18}F]FPBM on regional brain distribution in normal rats (at 120 min, average of n = 6), IDAM inhibits uptake into the hypothalamus, striatum, cortex and hippocampus.

* The data for [^{18}F]FPBM is reported previously[6].

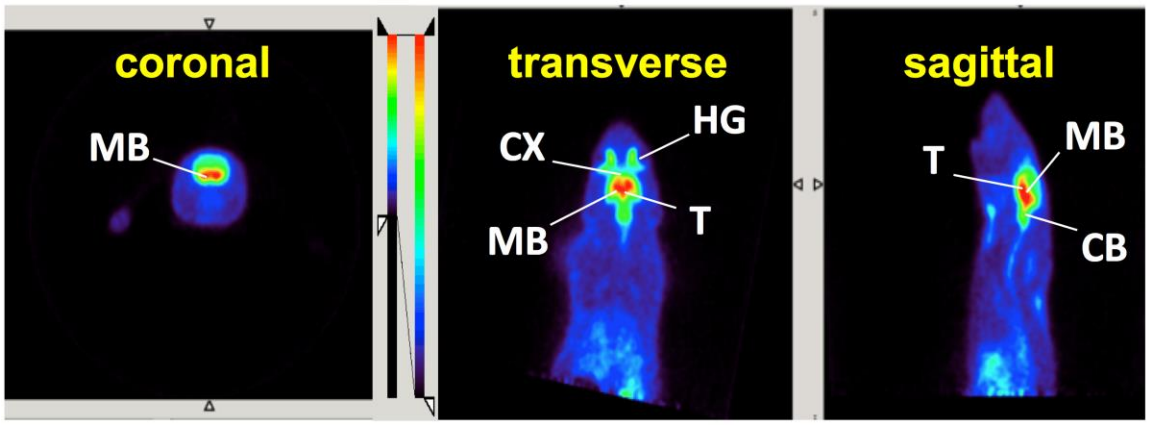

Fig. 5. While under isoflurane anesthesia, 55.5 MBq of [^{18}F]**1** was injected through a catheter placed into the tail vein of the rats and scanning commenced. A-PET images (coronal, transverse, and sagittal views) of [^{18}F]**1** localization in the rat brains reflect known areas of SERT distribution. Total scan time was 2 h. One time frame is shown (0 to 60 min). [^{18}F]**1** localized in the midbrain (MB), cortex (CX), and thalamus (T), which are regions where SERT binding sites are concentrated. Activity due to nonspecific binding was detected in the Harderian glands (HG); this nonspecific binding is commonly observed in rats and mice for other PET agents. Little uptake is observed in the cerebellum (CX), a region with low SERT density.

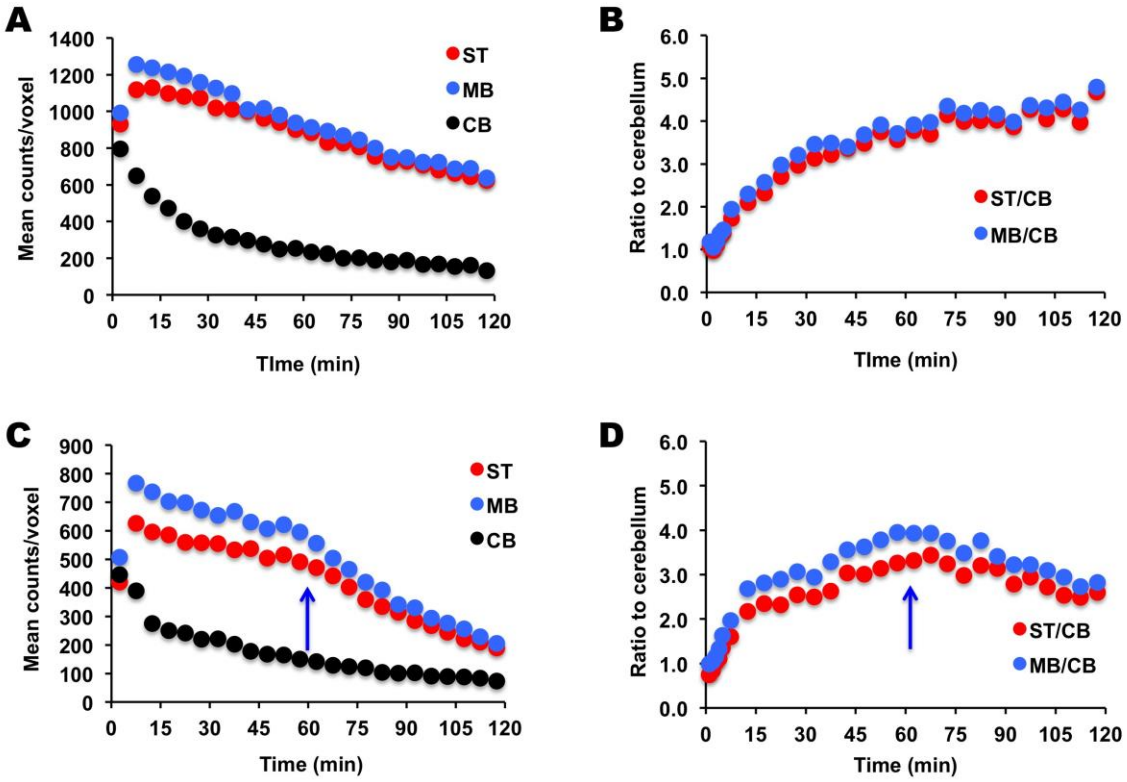

Fig. 6. Kinetic data of [^{18}F]**1** after injection into a rat. **A**: Activity of [^{18}F]**1** (55.5 MBq injection) in the striatum (ST), midbrain (MB), and cerebellum (CB) over time. **B**: Ratio of ST/CB and MB/CB over time. **C**: Activity of [^{18}F]**1** (40.7 MBq injection) in ST, MB, and CB over time. After 60 min, escitalopram (2 mg/kg) was injected into the rat. **D**: Ratio of ST/CB and MB/CB over time with escitalopram (2 mg/kg) IV injection after 60 min. Data were generated from A-PET image analysis using the AMIDE software. Values on the y-axis for graphs **A** and **C** are mean counts/voxel. **A**: After a 55.5 MBq injection of [^{18}F]**1**, the uptake peaked at 10 min and the activity counts in the non-target region, the cerebellum, rapidly decreased. **B**: The regions (of interest)-to-cerebellum ratio peaked at approximately 100 to 110 min after-IV injection. **C**: Intravenous injection of escitalopram (2 mg/kg) 60 min after a 40.7 MBq injection of [^{18}F]**1** (indicated by blue arrow) shows clear competition for SERT binding sites. Radioactivity in the target regions (ST and MB) decreased rapidly after escitalopram injection and reached

cerebellar activity levels by 150 min. **D**: A dramatic decrease in the regions (of interest)-to-cerebellum ratio was also observed.

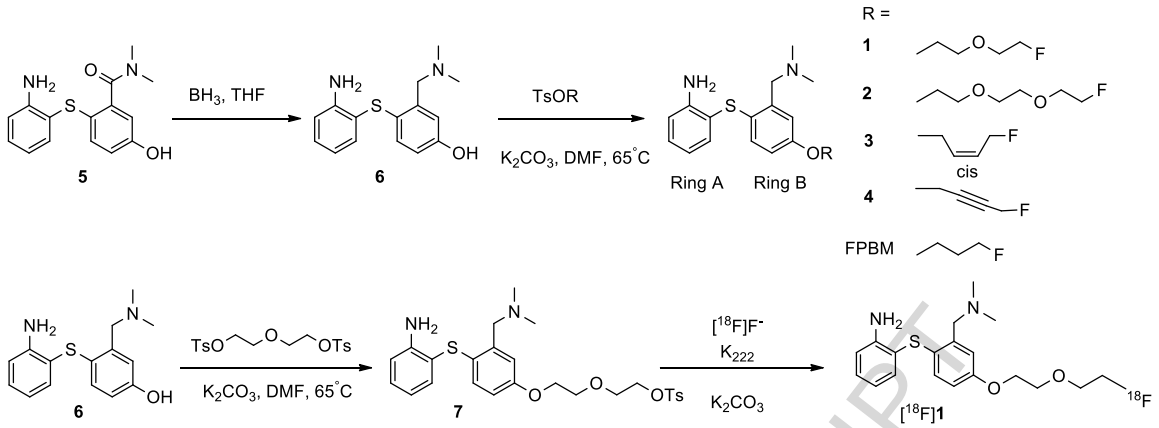

Scheme 1. Preparation of compounds **1**−**4** and the -OTs precursor **7** for ^{18}F radiolabeling. Several precursors of TsOR substituted groups were readily prepared according to the literature [34]

Table 1. Binding affinities of compounds **1**−**4** to SERT, DAT, and NET (average of n = 3, K_i ± SD, nM)*

Compound	R	Binding affinity (K_i, nM)			Selectivity	
		SERT	DAT	NET	DAT/SERT	NET/ SERT
1	$CH_2CH_2OCH_2CH_2F$	0.09 ± 0.01	370 ± 66	2.37 ± 0.25	4111	26.3
2	$CH_2CH_2OCH_2CH_2OCH_2CH_2F$	0.22 ± 0.02	586 ± 8	3.23 ± 0.40	2663	14.7
3	$CH_2CH=CHCH_2F$ (cis)	0.020 ± 0.003	686 ± 20	80 ± 11	34300	4010
4	$CH_2C\equiv CCH_2F$	0.40 ± 0.14	ND	ND	ND	ND

*In vitro binding studies were carried out using membrane homogenate preparations of LLC-PK1 cells overexpressing different types of monoamine transporters [36].

Table 2. Biodistribution of [^{18}F]**1** in male Sprague Dawley rats (average of n = 5, % dose/g ± SD)

Region	2 min	30 min	60 min	120 min
Heart	0.84 ± 0.12	0.32 ± 0.04	0.25 ± 0.06	0.15 ± 0.01
Liver	0.47 ± 0.11	0.38 ± 0.03	0.30 ± 0.04	0.25 ± 0.03
Spleen	0.55 ± 0.09	1.39 ± 0.11	1.11 ± 0.18	0.56 ± 0.12
Lung	5.47 ± 0.38	2.80 ± 0.54	2.60 ± 0.37	1.16 ± 0.27
Kidney	1.68 ± 0.31	1.33 ± 0.26	1.10 ± 0.32	0.81 ± 0.20
Pancreas	1.73 ± 0.66	0.36 ± 0.09	0.22 ± 0.04	0.18 ± 0.03
Skin	0.18 ± 0.05	0.32 ± 0.03	0.39 ± 0.03	0.35 ± 0.07
Bone	0.24 ± 0.06	0.23 ± 0.02	0.22 ± 0.03	0.18 ± 0.08
Muscle	0.37 ± 0.08	0.12 ± 0.01	0.12 ± 0.02	0.10 ± 0.02
Blood	0.43 ± 0.06	0.35 ± 0.05	0.34 ± 0.04	0.22 ± 0.04
Brain	1.04 ± 0.15	0.91 ± 0.08	0.86 ± 0.08	0.67 ± 0.08

Regional brain uptakes

	[^{18}F]**1**	[^{18}F]FPBM	[^{18}F]**1**	[^{18}F]FPBM	[^{18}F]**1**	[^{18}F]FPBM	[^{18}F]**1**	[^{18}F]FPBM
Hypothalamus	1.22 ± 0.17	1.15±0.11	1.55 ± 0.15	1.22±0.16	1.30 ± 0.20	1.08±0.21	1.20 ± 0.12	0.75±0.18
Striatum	1.04 ± 0.22	0.92±0.04	0.98 ± 0.09	0.90±0.17	1.02 ± 0.17	0.74±0.15	0.81 ± 0.15	0.46±0.10
Cortex	1.15 ± 0.20	1.05±0.07	1.02 ± 0.11	1.00±0.18	0.73 ± 0.25	0.98±0.18	0.66 ± 0.08	0.44±0.08
Hippocampus	1.07 ±0.19	0.89±0.06	0.93 ± 0.10	0.79±0.11	0.88 ± 0.11	0.65±0.12	0.77 ± 0.12	0.38±0.04
Cerebellum	0.87 ± 0.15	1.02±0.11	0.36 ± 0.03	0.35±0.05	0.32 ± 0.05	0.23±0.07	0.20 ± 0.02	0.10±0.02

Region-to-cerebellum ratio

	[^{18}F]**1**	[^{18}F]FPBM	[^{18}F]**1**	[^{18}F]FPBM	[^{18}F]**1**	[^{18}F]FPBM	[^{18}F]**1**	[^{18}F]FPBM
Hypothalamus	1.40 ± 0.12	1.14±0.15	4.15 ± 0.23	3.50±0.38	4.29 ± 0.28	4.69±0.74	6.10 ± 0.39	7.67±1.39
Striatum	1.20 ± 0.13	0.90±0.12	2.73 ± 0.20	2.58±0.30	3.21 ± 0.41	3.19±0.49	3.96 ± 0.69	4.67±0.29
Cortex	1.32 ± 0.09	1.03±0.12	2.61 ± 0.12	2.87±0.41	2.85 ± 0.13	4.26±0.96	3.25 ± 0.30	4.53±0.54
Hippocampus	1.23 ± 0.21	0.88±0.07	2.58 ± 0.22	2.26±0.25	2.89 ± 0.54	2.82±0.42	3.80 ± 0.69	3.87±0.50

* The biodistribution of [^{18}F]FPBM was previously reported [6].

Table 3. The effects of SERT and NET inhibitors on region-to-cerebellum ratios (at 120 min, average of n = 5): Escitalopram greatly decreased the region-to-cerebellum ratio and little to no inhibition was seen with nisoxetine.

	Hypothalamus	Striatum	Cortex	Hippocampus
Control	6.54 ± 0.82	4.40 ± 0.86	3.70 ± 0.70	3.84 ± 0.59
Nisoxetine	6.47 ± 0.48	4.03 ± 0.21	3.18 ± 0.23	3.51 ± 0.39
Escitalopram	2.09 ± 0.15	1.60 ± 0.51	1.23 ± 0.13	1.43 ± 0.11

References

[1] Bousman CA, Forbes M, Jayaram M, Eyre H, Reynolds CF, Berk M, et al. Antidepressant prescribing in the precision medicine era: a prescriber's primer on pharmacogenetic tools. BMC Psychiatry 2017;17:60.
[2] Kambeitz JP and Howes OD. The serotonin transporter in depression: Meta-analysis of in vivo and post mortem findings and implications for understanding and treating depression. J Affect Disord 2015;186:358-66.
[3] Spies M, Knudsen GM, Lanzenberger R, and Kasper S. The serotonin transporter in psychiatric disorders: insights from PET imaging. Lancet Psychiatry 2015;2:743-55.
[4] Oya S, Choi S, Kung M, and Kung H. 5-Chloro-2-(2'-((dimethylamino)methyl)-4'-iodophenylthio)benzenamine: a new serotonin transporter ligand. Nucl Med Biol 2007;34:129-39.
[5] Kung H, Newman S, Choi S, Oya S, Hou C, Zhuang Z, et al. 2-(2-(dimethylaminomethyl)phenoxy)-5-iodophenylamine: an improved serotonin transporter imaging agent. J Med Chem 2004;47:5258-64.
[6] Wang JL, Parhi AK, Oya S, Lieberman B, Kung MP, and Kung HF. 2-(2'-((Dimethylamino)methyl)-4'-(3-[(18)F]fluoropropoxy)-phenylthio)benzenamine for positron emission tomography imaging of serotonin transporters. Nucl Med Biol 2008;35:447-58.
[7] Wang JL, Deutsch EC, Oya S, and Kung HF. FlipADAM: a potential new SPECT imaging agent for the serotonin transporter. Nucl Med Biol 2010;37:577-86.
[8] Mavel S, Meheux N, Guilloteau D, and Emond P. Synthesis and in vitro evaluation of fluorinated diphenyloxide derivatives and sulfur analogs as serotonin transporter ligands. Bioorg Med Chem 2010;18:236-41.
[9] Jarkas N, Voll RJ, Williams L, and Goodman MM. Validation of two fluoro-analogues of N,N-dimethyl-2-(2'-amino-4'-hydroxymethyl-phenylthio)benzylamine as serotonin transporter imaging agents using microPET. Nucl Med Biol 2010;37:593-603.
[10] Kang HH, Wang CH, Chen HC, Li IH, Cheng CY, Liu RS, et al. Investigating the effects of noise-induced hearing loss on serotonin transporters in rat brain using 4-[(18)F]-ADAM/small animal PET. Neuroimage 2012.
[11] Chen YA, Huang WS, Lin YS, Cheng CY, Liu RS, Wang SJ, et al. Characterization of 4-[18F]-ADAM as an imaging agent for SERT in non-human primate brain using PET: a dynamic study. Nucl Med Biol 2012;39:279-85.
[12] Hesse S, Brust P, Mading P, Becker GA, Patt M, Seese A, et al. Imaging of the brain serotonin transporters (SERT) with (18)F-labelled fluoromethyl-McN5652 and PET in humans. Eur J Nucl Med Mol Imaging 2012;39:1001-11.
[13] Paterson LM, Kornum BR, Nutt DJ, Pike VW, and Knudsen GM. 5-HT radioligands for human brain imaging with PET and SPECT. Med Res Rev 2013;33:54-111.
[14] Huang WS, Huang SY, Ho PS, Ma KH, Huang YY, Yeh CB, et al. PET imaging of the brain serotonin transporters (SERT) with N,N-dimethyl-2-(2-amino-4-[18F]fluorophenylthio)benzylamine (4-[18F]-ADAM) in humans: a preliminary study. Eur J Nucl Med Mol Imaging 2013;40:115-24.

[15] Szabo Z, Kao PF, Scheffel U, Suehiro M, Mathews WB, Ravert HT, et al. Positron emission tomography imaging of serotonin transporters in the human brain using [^{11}C](+)McN5652. Synapse 1995;20:37-43.
[16] Zessin J, Eskola O, Brust P, Bergman J, Steinbach J, Lehikoinen P, et al. Synthesis of S-([18F]fluoromethyl)-(+)-McN5652 as a potential PET radioligand for the serotonin transporter. Nucl Med Biol 2001;28:857-63.
[17] Stehouwer JS and Goodman MM. (11) C and (18) F PET radioligands for the serotonin transporter (SERT). J Labelled Comp Radiopharm 2013;56:114-9.
[18] Newberg A, Plossl K, Mozley P, Stubbs J, Wintering N, Udeshi M, et al. Biodistribution and imaging with (123)I-ADAM: a serotonin transporter imaging agent. J Nucl Med 2004;45:834-41.
[19] Newberg AB, Amsterdam JD, Wintering N, Ploessl K, Swanson RL, Shults J, et al. 123I-ADAM binding to serotonin transporters in patients with major depression and healthy controls: a preliminary study. J Nucl Med 2005;46:973-7.
[20] Wilson AA, Ginovart N, Schmidt M, Meyer JH, Threlkeld PG, and Houle S. Novel radiotracers for imaging the serotonin transporter by positron emission tomography: synthesis, radiosynthesis, and in vitro and ex vivo evaluation of ^{11}C-labeled 2-(phenylthio)araalkylamines. J Med Chem 2000;43:3103-10.
[21] Wilson AA, Ginovart N, Hussey D, Meyer J, and Houle S. In vitro and in vivo characterisation of [^{11}C]-DASB: a probe for in vivo measurements of the serotonin transporter by positron emission tomography. Nucl Med Biol 2002;29:509-15.
[22] Kupers R, Frokjaer VG, Erritzoe D, Naert A, Budtz-Joergensen E, Nielsen FA, et al. Serotonin transporter binding in the hypothalamus correlates negatively with tonic heat pain ratings in healthy subjects: a [11C]DASB PET study. Neuroimage 2011;54:1336-43.
[23] Ginovart N, Sun W, Wilson AA, Houle S, and Kapur S. Quantitative validation of an intracerebral beta-sensitive microprobe system to determine in vivo drug-induced receptor occupancy using [11C]raclopride in rats. Synapse 2004;52:89-99.
[24] Frick A, Ahs F, Engman J, Jonasson M, Alaie I, Bjorkstrand J, et al. Serotonin Synthesis and Reuptake in Social Anxiety Disorder: A Positron Emission Tomography Study. JAMA Psychiatry 2015;72:794-802.
[25] Kim E, Howes OD, Park JW, Kim SN, Shin SA, Kim BH, et al. Altered serotonin transporter binding potential in patients with obsessive-compulsive disorder under escitalopram treatment: [11C]DASB PET study. Psychol Med 2015:1-10.
[26] Oya S, Choi SR, Coenen H, and Kung HF. New PET imaging agent for the serotonin transporter: [(18)F]ACF (2-[(2-amino-4-chloro-5-fluorophenyl)thio]-N,N-dimethyl-benzenmethanamine). J Med Chem 2002;45:4716-23.
[27] Huang Y, Bae SA, Zhu Z, Guo N, Roth BL, and Laruelle M. Fluorinated diaryl sulfides as serotonin transporter ligands: synthesis, structure-activity relationship study, and in vivo evaluation of fluorine-18-labeled compounds as PET imaging agents. J Med Chem 2005;48:2559-70.
[28] Shiue G, Choi S, Fang P, Hou C, Acton P, Cardi C, et al. N,N-dimethyl-2-(2-amino-4-(18)F-fluorophenylthio)-benzylamine (4-(18)F-ADAM): an improved PET radioligand for serotonin transporters. J Nucl Med 2003;44:1890-7.
[29] Cheng CY, Chou TK, and Shiue CY. Fully automated one-pot two-step synthesis of 4-[(18)F]-ADAM, a potent serotonin transporter imaging agent. Appl Radiat Isot 2016;110:8-15.

[30] Wang J, Parhi A, Oya S, Lieberman B, and Kung H. In vivo characterization of a series of 18F-diaryl sulfides (18F-2-(2'-((dimethylamino)methyl)-4'-(fluoroalkoxy)phenylthio)benzenamine) for PET imaging of the serotonin transporter. J Nucl Med 2009;50:1509-17.
[31] Wang J, Oya S, Parhi A, Lieberman B, Ploessl K, Hou C, et al. In vivo studies of the SERT-selective [18F]FPBM and VMAT2-selective [18F]AV-133 radiotracers in a rat model of Parkinson's disease. Nucl Med Biol 2010;37:479-86.
[32] Qiao H, Zhang Y, Wu Z, Zhu L, Choi SR, Ploessl K, et al. One-step preparation of [(18)F]FPBM for PET imaging of serotonin transporter (SERT) in the brain. Nucl Med Biol 2016;43:470-7.
[33] Zhu L, Li G, Choi SR, Plossl K, Chan P, Qiao H, et al. An improved preparation of [18F]FPBM: A potential serotonin transporter (SERT) imaging agent. Nucl Med Biol 2013;40:974-9.
[34] Maisonial A, Billaud EMF, Besse S, Rbah-Vidal L, Papon J, Audin L, et al. Synthesis, radioiodination and in vivo screening of novel potent iodinated and fluorinated radiotracers as melanoma imaging and therapeutic probes. Eur J Med Chem 2013;63:840-53.
[35] Gu H, Wall SC, and Rudnick G. Stable expression of biogenic amine transporters reveals differences in inhibitor sensitivity, kinetics, and ion dependence. J Biol Chem 1994;269:7124-30.
[36] Choi S, Hou C, Oya S, Mu M, Kung M, Siciliano M, et al. Selective in vitro and in vivo binding of [(125)I]ADAM to serotonin transporters in rat brain. Synapse 2000;38:403-12.
[37] Loening AM and Gambhir SS. AMIDE: A Free Software Tool for Multimodality Medical Image Analysis. Mol Imaging 2003;2:15353500200303133.
[38] Kung MP, Hou C, Oya S, Mu M, Acton PD, and Kung HF. Characterization of [^{123}I]IDAM as a novel single-photon emission tomography tracer for serotonin transporters. Eur J. Nucl Med 1999;26:844-53.
[39] Heinz H. Coenen, Antony D. Gee, Michael Adam, Gunnar Antoni , Cathy S. Cutler, Yasuhisa Fujibayashi, et al. Consensus nomenclature rules for radiopharmaceutical chemistry — Setting the record straight. Nucl Med Bio 2017; 55:v–xi.